Research Article

SOHAG JOURNAL OF SCIENCES

https://doi.org/10.21608/sjsci.2025.419164.1307

Investigation of Maximum Depth for Cherenkov Radiation at Energies above 10^{14} eV

Kadhom F. Fadhel

Directorate General of Education in Diyala, Ministry of Education, Baghdad, Iraq
**Email: kadhumfakhry@uomustansiriyah.edu.iq*

Received: 31st Augest 2025 **Revised:** 4th October 2025 **Accepted:** 5th October 2025
Published online: 24th November 2025

Abstract: The CORSIKA code will be used to simulate a part of an Extensive Air Shower (EAS) that describes the lateral distribution function (LDF) with the Yakutsk array for Cherenkov photons. The EAS development has been estimated for several primary particles including oxygen, helium, and proton (O2, He, and H) in the vicinity of the knee region of the cosmic ray energy spectrum with energies above 10^{14} eV for zenith angles $\leq 50^{\circ}$. The several shower beam simulations of the mentioned particles were performed at high energies for different vertical and inclined zenith angles. One of the purposes of the work is the reconstruction of Cherenkov photons LDF by depending on the Peak Function (Gauss Mod) through a parameterization as a function of the zenith angle, using the Yakutsk array for several primary particles at various zenith angles for air shower observables. At energies above 10^{14} eV, the calculated lateral distribution function of Cherenkov photons aligns closely with the experimental data from the Yakutsk array.
Keywords: Cosmic Ray, Cherenkov Radiation, Gauss Function, CORSIKA Code.

1. Introduction

Research in the field of astrophysics concerning cosmic rays with energies above 0.1 EeV is crucial to understanding the universe's operations and evolution [1]. One of the major unsolved issues in astroparticle physics is locating and comprehending the sources of high-energy cosmic rays [2]. Only by knowing the mass composition of cosmic rays can the long-standing riddle of the formation of high-energy cosmic rays be solved. The mass distribution provides strong constraints on cosmic ray acceleration and propagation through the galactic and extragalactic Universe. Particularly interesting are measurements of the mass composition close to structures visible in the cosmic ray energy spectrum [3,4]. which is detectable for energy over roughly 10^{14} eV in ground-based detector arrays. These particles are at the upper end of the energy spectrum and have the highest energy of any known particle in the universe [5]. As a result, there is a lot of interest in the issues surrounding their origin and mass composition, and cosmic-ray air showers are seen at observatories worldwide [6]. Cosmic particles are continually present in the Earth's atmosphere. These high-energy particles origins and acceleration methods remain unclear. One of the most important factors in this area of research represents the cosmic ray mass composition. This parameter aids in understanding the origin, the acceleration process, and the propagation from the origin to Earth [7]. Charged particles travel randomly across space due to the chaotic galactic magnetic fields. As a result, charged particles are unable to locate their origins, with the exception of ultra-high energy particles. Thus, to understand the nature of cosmic rays, one must be aware of their energy spectrum as well as mass composition [8,9]. Ultra-high-energy charged particles cosmic rays are defined as those with an energy greater than 10^{18} eV. Investigating these particles and their origins is crucial because it can provide critical details about cosmic accelerators that help us comprehend the universe. When a sufficiently energetic cosmic rays particle enters the Earth's atmosphere, a series of secondary particles known as EAS are created [10]. Investigating the traits of EAS produced by cosmic rays with extremely high energies cosmic rays is essential. Furthermore, showers of chain reactions generated by electromagnetic gamma rays and elementary particles in the Earth's atmosphere have been used to detect high energy cosmic ray [11]. Since some major particles are not immediately visible, they need to be examined based on the showers in EAS that were measured in various ways. Due to their incredibly low taxes, the Ultra High Energy Cosmic Rays (UHECR) that reach the Earth cannot be directly observed in space [12]. These particles interact with atmospheric molecules as they enter the atmosphere, causing secondary particles known as EAS. There are millions of collisions and secondary particle decay in the EAS caused by cosmic rays or cosmic rays with extremely high energies [13]. These showers can be seen with fluorescence detectors, which can track energy depositions as they grow along the atmosphere, or surface detectors, which track depositions as the particles hit the ground [14]. One of the main EAS aspects that large ground-based air shower arrays can measure with exceptional accuracy is the local particle density of the charged at various distances from the shower center. Comparing experimental data with the results of EAS simulations is the only trustworthy method for figuring out the basic energy spectrum and composition of cosmic rays as well as validating hadronic interaction models at extremely high energies [15]. For this reason, accurate theoretical predictions on the LDF of the main EAS components throughout a broad range of radial distances are crucial for future experiment design studies in the field of CR research as well as the physical interpretation of earlier experimental results [16]. Comprehensive information about the experimental setup and simulation technique detection in EAS has been obtained through processing and analysis of experimental data. The Monte Carlo approach, which can be used to deduce the primary particle energy type and shower axis from the LDF characteristics of secondary charged particles, is one of the most significant numerical simulation techniques for investigating EAS features [17]. This array enables systematic analysis of the energy spectrum as well as mass composition of CR in the energy range above 10^{14} eV. The depth of the EAS maximum Xmax could be determined by looking at the EAS LDF and temporal structure [18]. In this study, the CORSIKA simulation engine (v.6.0, QGSJet-II.04 model) was used to simulate hadronic processes of the EAS showers of LDF for circumstances and configurations of the Yakutsk EAS array [19]. The outcomes of the numerical simulation of LDF density were estimated using the Gauss Function, a technique for characterizing the lateral distribution of the showers, and its applicability to reconstructing the events documented in Yakutsk was investigated. The primary benefit of this method is its ability to recapture LDF events that were seen using the Yakutsk array. An outstanding chance for primary particle identification, mass composition, and energy characterization around the knee and ankle regions has been demonstrated by comparing the estimated LDF density of Cherenkov photons with the reconstructed EAS showers captured with the Yakutsk EAS array.

2. Materials and methods

In this article, the evolution of the atmospheric cascade for the LDF photon flux for Cherenkov is predicted to use a hadron interaction model, QGSJET, for the CORSIKA simulation. CORSIKA cosmic ray simulations are the most popular instrument for simulating atmospheric cascades [20]. Numerous hadrons, electrons, photons, muons, and nuclei in the atmosphere are simulated in the program, along with their interactions and decays. Secondary particles that are unstable are monitored as they move through the atmosphere until they decay or come into contact with air nuclei. At a preset altitude above sea level, the simulations provide accurate information on the energy, type, momentum, position, and arrival time of generated secondary particles. The light, medium, heavy, and proton up to iron are among the primary particles that can be taken into consideration. At Oktyomtsy, near Yakutsk, Russia, the Yakutsk array is located 100 meters above sea level (1020 g cm^{-2}) (61.7~N, 129.4~E). Particularly for hadronic cascades with energy at the "knee," this observation level is rather close to the EAS shower maximum. The differences in shower development are therefore less pronounced than at lower observation levels. This makes it possible for the models to generate flatter distributions of the different components of the EAS shower, particularly the air Cherenkov light flux. [21].

3.CORSIKA Simulation

When the resulting air shower develops in the atmosphere as a result of the interactions of CR with the nuclei of atmospheric atoms, it is difficult to analyze the data directly without a simulation process. Simple analytical models cannot adequately capture the complexities of shower evolution. Furthermore, for precise shower modeling progression, the MC simulation of particle interaction and transport must be carried out. Recently, MC packages have been used to simulate EAS using CORSIKA an event generator that uses the hadronic interaction model QGS_{Jet}-II.04 [21,22]. In order to change the contests and the amount of the data collection in accordance with preset regulations, the air shower simulation algorithm, which consist of several interconnected processes, require a data collection with a variable number of records. The CORSIKA simulation engine's internal control algorithms continuously track and report particles that come into contact between the ground and injection phases, either with the ground or over specified observation surfaces. Knowing the number of showers allows one to identify the primary particle and understand how its energy interacts with atmospheric atoms. Electron, muon, and gamma ray kinetic energy are then defined along with the task name. Following the definition of the zenith angle and the thinning energy, the detection levels are chosen for the matrix that will be utilized later. The shower progress is directly influenced by the diffractive interactions. Additionally, charting shower densities against the atmosphere's shower core at specific energies above 10^{14} eV amply validates that fact. The graphs were plotted using the data obtained from simulations conducted for the hadronic interaction model QGS_{Jet}-II.04 using the CORSIKA system. The increase of the LDF Cherenkov flux photons of the resulting extremely high-energy secondary CRs reacts with the atmosphere and arranges the total correlated production data. The creation of oxygen, helium, and protons from air showers in the primary energy range above 10^{14} eV was investigated using the simulation. The observation level was assumed to above sea level (1020 g cm^{-2}), this is equivalent to the Yakutsk Cosmic Rays Station. During the simulations, the ordinary environment was used. Particularly for the hadronic cascades with energy surrounding the "knee," this observation level is close to shower maximum. Because of this, shower development fluctuations are less significant than at lower observation altitudes. This enables the models to produce flatter distributions of the various shower components, specifically the air Cherenkov light flux. The simulated particles are primary oxygen, helium, and proton. As a result of the significant reduce of the statistical fluctuations is achieved, and as the obtained lateral distribution of Cherenkov light flux densities in EAS is with less uncertainties, comparing to previous work. When performing the simulation, the number of photons in the wavelength period (λ_1 = 300 nm, λ_2 = 400 nm) emitted in the radiator was taken into account.

Internal control procedures in CORSIKA simulation engine continuously check and report particles touching the ground and/or moving over predetermined observing surfaces between the ground and injection stages. When the quantity of showers is established, the elementary particle's identification is ascertained, and its energy can interact with atmospheric atoms. The task name and the kinetic energy of electrons, muons, and gamma rays are then defined. We next select the observing levels for the array to be employed after defining the zenith angle and the thinning energy. Finally, we give the secondary particles that come from the chain reaction a name. The shower progress is directly impacted by the diffractive interactions. Additionally, plotting the density of showers represented on the Y axis against the atmosphere's shower core represented on the

X axis at specific energies above 10^{14} eV amply validates that fact. Plotting of the graphs was based on data received from simulations run using the CORSIKA system.. The table 1 shows the data entry process for the CORSICA software when running a simulation.

Table 1. CORSIKA input card Used.

Number of run/ events	001300
Number of first shower event	100400
Primary particle code	402/ 14/1608
QGS_{Jet}-II.04	T 0
Cherenkov detector grid	10 8 1200 1500 80 50
Cherenkov wavelength band	300-400 nm
thinning	10^{-6}
observation level	1020 g cm^{-2}
Energy range of primary	above 10^{14} eV
Range zenith angle	angles ≤ 50˚

The CORSIKA simulation of two primary particles, a proton and an oxygen, for various zenith angles is displayed in Figure 1 together with the Cherenkov photons in EAS generated by various elementary particles in the energy above 10^{14} eV. The figure shows that the air shower develops more and wider when the angle is 0˚, and the number of particles produced decreases as the zenith angle increases. The CORSIKA code simulation for energies between 10^{15} and 10^{19} eV for a number of primary particles, including the proton, helium, and oxygen, is displayed in Figure 2. The "knee" area displayed the obtained LDF of atmospheric LDF of photon flux for Cherenkov originating from different CR nuclei. Demonstrate how the Yakutsk array affects the zenith angles for LDF for Cherenkov photons for a range of primary particles, including oxygen, proton, and helium, for different primary energies in the simulation.

4. Results and Discussion:

4.1. Parameterization of Cherenkov Radiation

The Cherenkov photon result in EAS is approximated using a variety of parameterizations, and the majority of reconstruction techniques are predicated on a certain assumption. Reconstructing main particle characteristics and event analysis require practical parameterization. The results for a number of simple particle approximations are displayed in Figure 2. Furthermore, the EAS of air Cherenkov flux photons generated by oxygen, helium, and proton is estimated using the proposed parameterization. The following parameters for the primary particles were generated by parameterizing the Cherenkov light of showers that originated in the EAS using a Peak Function (Gauss Mod):

$$Q_{(\theta)} = \beta_0 + \frac{\gamma}{\delta_0} exp^{\frac{1}{2}(\frac{\sigma}{\delta_0})^2} \int_{-\infty}^{z} \frac{1}{\sqrt{2\pi}} exp^{-\frac{y^2}{2}} dy \qquad (1)$$

when Q is the density of the EAS showers as a function of the zenith angle: $\beta_0, \gamma, \delta_0, and\ \sigma$ are obtained coefficients for Cherenkov photons EAS (see Table 2). These coefficients are obtained by fitting the CORSIKA results, which are given by the polynomial form:

$$K(\theta) = a_o + a_1(\theta) + a_2(\theta)^2 + a_3(\theta)^3 \qquad (2)$$

where $K(\theta) = \beta_0, \gamma, \delta_0, and\ \sigma$ the parameters of Eq. (2) as a function of the zenith angle and a_o, a_1, a_2 and a_3 there are their coefficients (see Table 2).

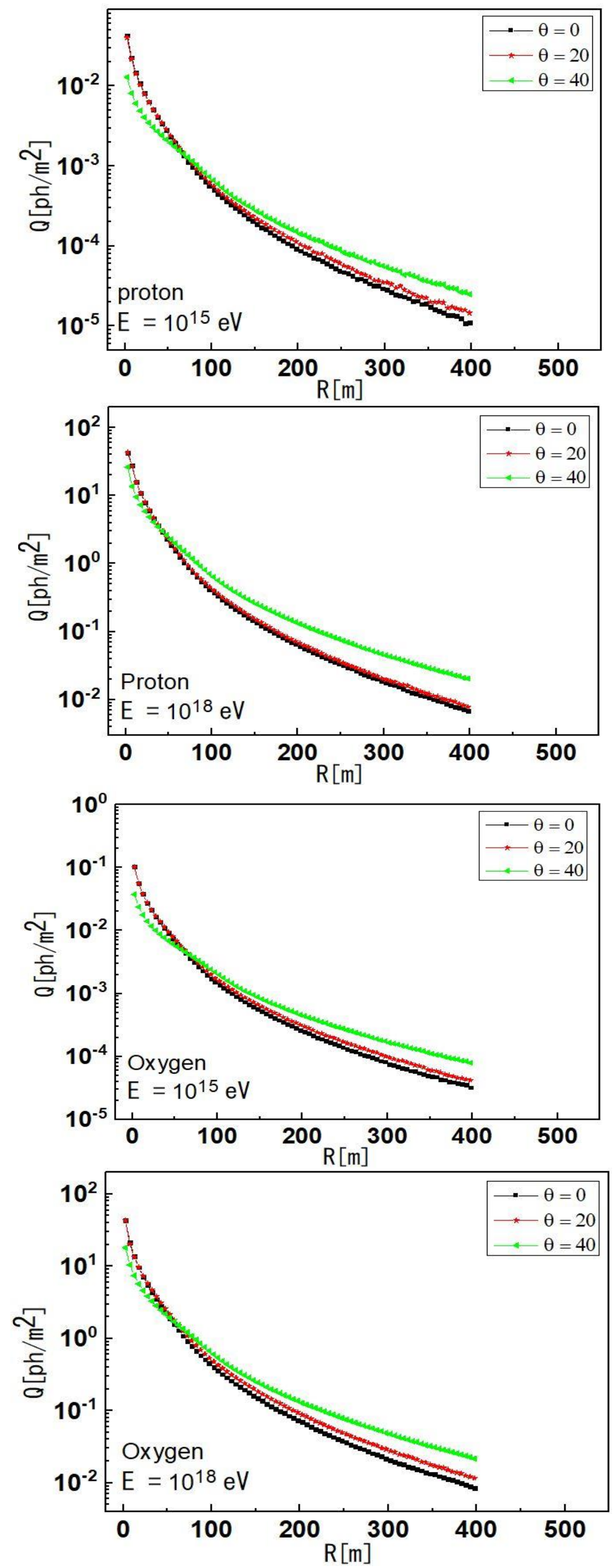

Fig. 1. demonstrates the difference between the zenith angle for primary particles oxygen and a proton using the CORSIKA code at the energies 10^{15} and 10^{18} eV.

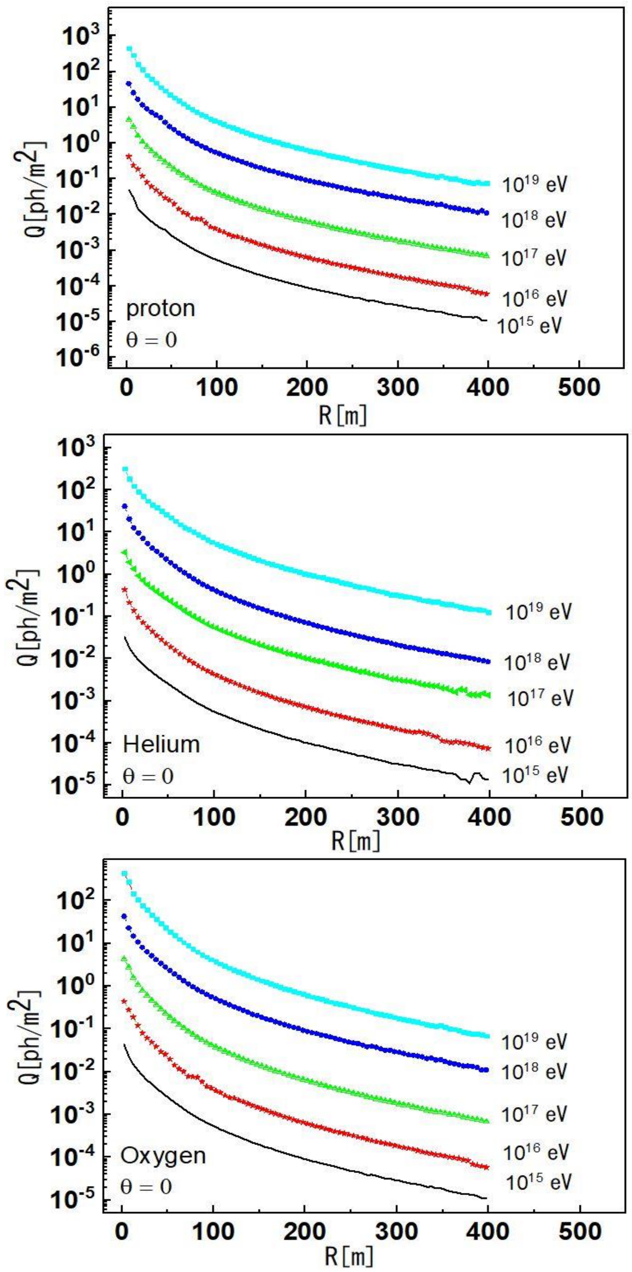

Fig. 2. Shows the difference between primary energy for primary particles helium, oxygen, and a proton using the CORSIKA code at the zenith angle (0) and energy range (10^{15} to 10^{19}) eV.

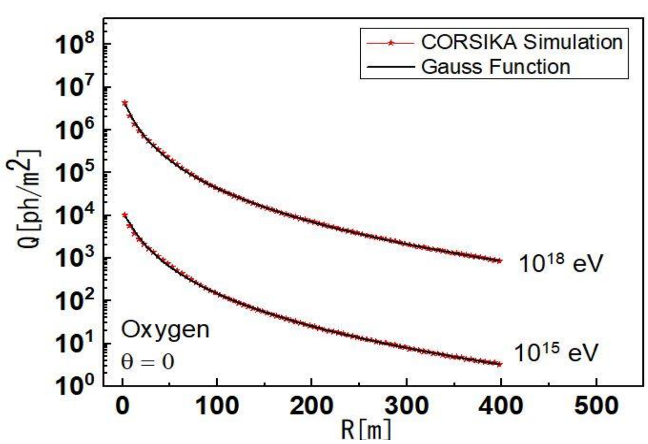

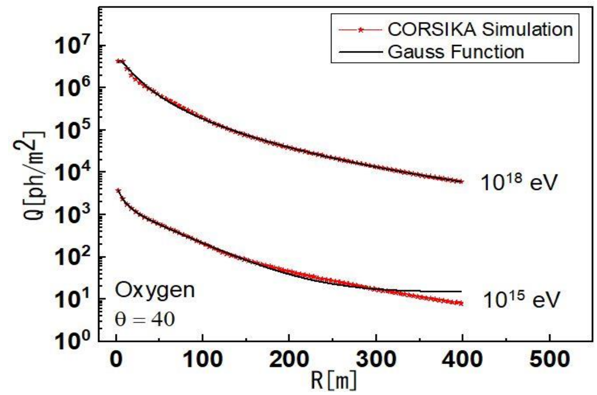

Fig. 3. The CORSIKA code (symbol line) and a Gauss function (solid line) simulation of Cherenkov photons LDF for primary energies (10^{15} and 10^{18} eV) with the two zenith angles for oxygen as a primary particle are compared.

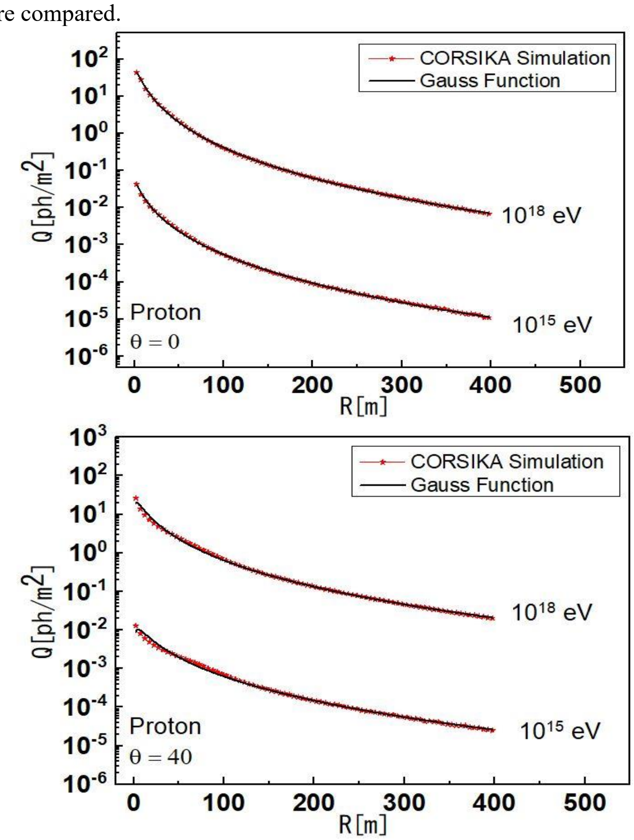

Fig. 4. The two zenith angles for proton as a primary particle are compared between a Gauss function (solid line) and the CORSIKA code (symbol line) simulation of Cherenkov photons LDF for primary energies (10^{15} and 10^{18} eV).

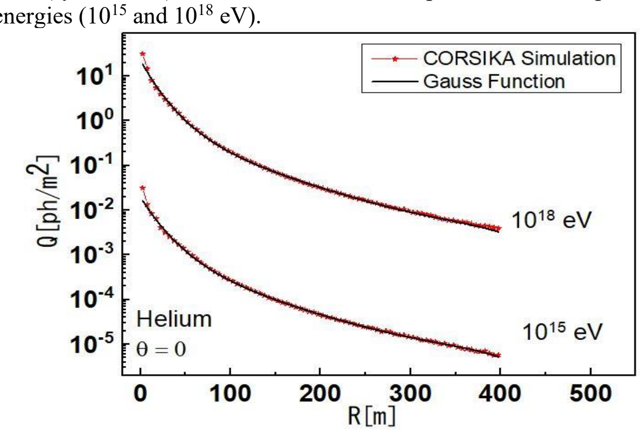

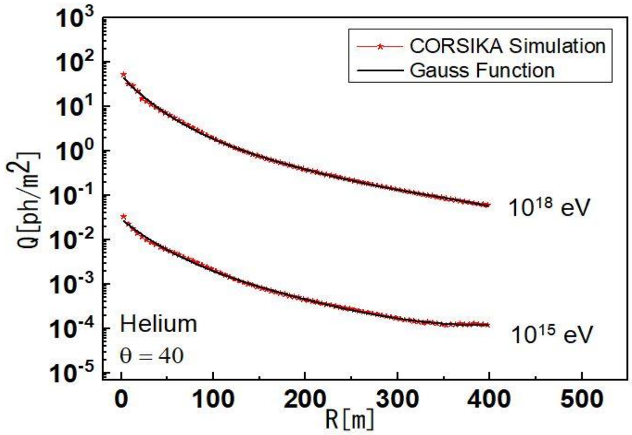

Fig. 5. The CORSIKA code (symbol line) and a Gauss function (solid line) simulation of Cherenkov photons LDF for primary energies (10^{15} and 10^{18} eV) with the two zenith angles for helium as a primary particle are compared.

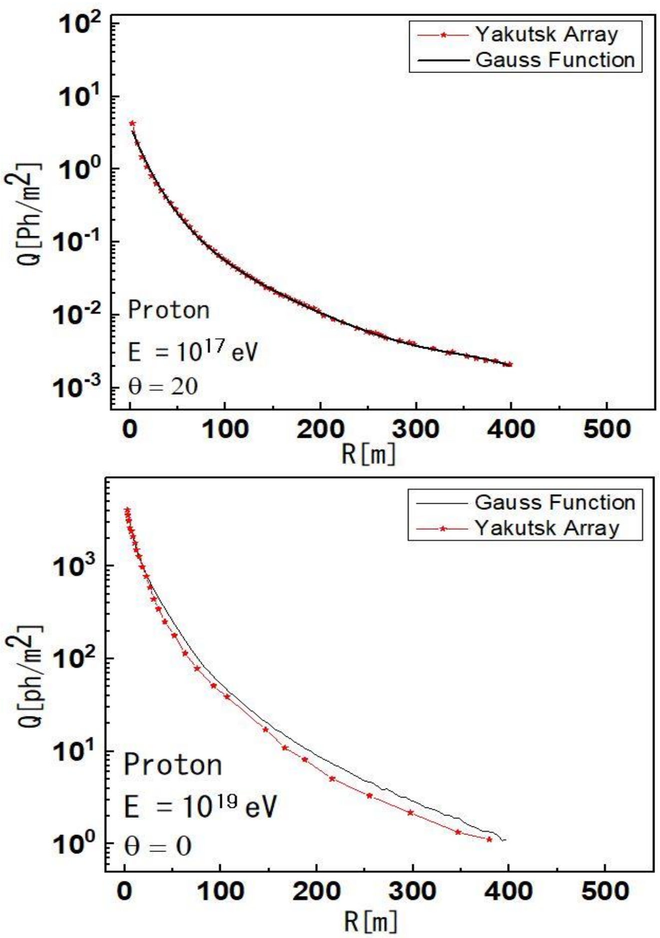

Fig. 6. Comparison of the Yakutsk EAS array (dashed line) measurement of the proton primary particle at energies 10^{17} and 10^{19} eV with the parametrized LDF of photon flux for Cherenkov (solid line) determined by the Gauss function.

Figures 3, 4, and 5 show the parameterization of Cherenkov photons LDF calculated with a Gauss function as a function of the zenith angle in an EAS shower. Within the two primary energies 10^{15} and 10^{18} eV, and two zenith angles (0˚, 40˚) Regarding some essential particles, including oxygen, helium, and protons. By observing the figures, we see that the curves of the Gauss Function agree to a large extent with the Corsica simulation data for the mentioned particles through the analysis of the function as shown in the table above.

4.2. Comparison of Parametrized LDF with the Experimental Data

The dynamic field of CR astrophysics, at the forefront of fundamental study, is studied by the Yakutsk EAS array CR of very high energy. Reconstructing the astrophysical features of the energy spectrum, including intensity, mass composition, primaries, and origin, and studying the elementary particle cascades in the atmosphere that are started by primary particles are the two main objectives to be accomplished in order to construct the Yakutsk array. Important parameters for EAS measurements include individual LDF, primary energy, shower core location, zenith angles, and the density of photon flux for Cherenkov. Figure 6 shows a comparison between the approximated Cherenkov photons (solid line) and those measured by the Yakutsk array (dashed line), indicating the feasibility of reconstructing the types of EAS primary particles. Gauss Function and experimental data for the Yakutsk system are in good accord. at the zenith angles (0˚, 20˚) for the proton main particle with energies 10^{17} and 10^{19} eV.

5. Conclusion

Several atmospheric characteristics and their effects on the atmospheric Cherenkov technique in general have been discussed. As it happens, a few of these parameters merit greater consideration in theoretical study. The initial oxygen, helium, and proton in EAS particles cause the LDF of the Cherenkov photon in the energy above 10^{14} eV has been modeled using the CORSIKA code. These simulations led to the employment of a Gauss Mod approximation function for a zenith angles < 50˚ and various main particles. By comparing the LDF Cherenkov photon estimations with those obtained with the Yakutsk array, the particle responsible for EAS showers is identified and its energy in the knee area of the CR spectrum is determined. The main advantage of the proposed method is its speedy assembly of a representative library of LDF patterns that may be evaluated to investigate real-world events recorded by EAS arrays and to reproduce the fundamental CR energy spectrum as well as mass composition.

CRediT authorship contribution statement:

No authors with me in this manuscript.

Data availability statement

I have all the data and it's ready at any time.

Declaration of competing interest

The authors declare that they have no known competing financial interests or personal relationships that could have appeared to influence the work reported in this paper.

Acknowledgments

Thanks to the Corsica Group and to the Directorate General of Education in Diyala, Ministry of Education, Baghdad, Iraq.

Table 2. By setting up the CORSIKA code simulation parameters of oxygen, helium, and proton primary particles at energies above 10^{15} eV and zenith angles ≤ 70˚, the coefficients of the Peak Function (Gauss Mod) (Eq.1).

Primary particles	$K(\theta)$	Coefficients				
		a_o	a_1	a_2	a_3	R^2
O_2	β_0	9.28×10^{6}	4.08×10^{-10}	4.89×10^{-30}	481.89	0.99435
	γ	297.07	1.46×10^{-16}	-1.35×10^{-35}	62.1	0.98752
	δ_0	35.53	2.5×10^{-17}	-2.36×10^{-36}	445.26	0.99056
	σ	963402.16	9.02×10^{-13}	2.71×10^{-31}	29289.72	0.99610
He	β_0	280.65	1.98×10^{-16}	-1.87×10^{-35}	438.22	0.97999
	γ	78.16	5.57×10^{-17}	-5.39×10^{-36}	106.43	0.99889
	δ_0	33668.68	5.22×10^{-13}	3.06×10^{-32}	264977.32	0.99081
	σ	65080.05	7.56×10^{-12}	-1.81×10^{-31}	5.46×10^{6}	0.99811
H	β_0	1.22×10^{6}	4.64×10^{-10}	5.45×10^{-30}	337.58	0.98909
	γ	321.16	5.32×10^{-18}	2.94×10^{-37}	44.95	0.99117
	δ_0	37.75	1.99×10^{-18}	-1.12×10^{-37}	1777.72	0.99449
	σ	55072.2	8.51×10^{-12}	-4.124×10^{-31}	116970.83	0.99284

References

[1] A. A. Watson, *Nucl. Phys. B-Proceedings Suppl*., 212(2011) 13–19.

[2] K. F. Fadhel and A. A. Al-Rubaiee, *arXiv Prepr. arXiv,* 2201 (2022) 01368.

[3] N. Akchurin et al., *Nucl. Instruments Methods Phys.* Res. Sect, 548 (2005) 336–354.

[4] S. Knurenko and I. Petrov, *Adv. Sp. Res.,* 64(2019) 2570–2577.

[5] A. Mishev, *Int. Sch. Res. Not.,*2012 (2012) 906358.

[6] A. R. Bell, *Astropart. Phys.,* 43 (2013) 56–70.

[7] A. A. Al-Rubaiee, O. A. Gress, K. S. Lokhtin, Y. V Parfenov, and S. I. Sinegovskii, *Russ. Phys. J.,* 48 (2005) 1004–1011.

[8] G. Agnetta et al., *Nucl. Instruments Methods Phys,* 570(2007). 22–35.

[9] S. Ogio et al., *Astrophys. J.,*612 (2004) 268.

[10] Y. Tsunesada et al., *Proc. 31st ICRC, Łódz,* 2009.

[11] S. P. Knurenko and I. Petrov, *JETP Lett.,*104 (2016) 297–301.

[12] N. M. Budnev et al., *arXiv Prepr. astro-ph/0511215*, (2005).

[13] V. V Prosin et al., *in EPJ Web of Conferences, EDP Sciences,* 2015, p. 4002.

[14] I. Rasekh and D. Purmohammad, *Astropart. Phys.,* 132 (2021) 102619.

[15] J. Knapp, D. Heck, S. J. Sciutto, M. T. Dova, and M. Risse, *Astropart. Phys.,*19 (2003) 77–99.

[16] A. A. Al-Rubaiee, Y. Al-Douri, and U. Hashim, *J. Astrophys.,* 2014(2014) 492814.

[17] B. Bartoli et al., *Astropart. Phys.,* 93 (2017) 46–55.

[18] J. Espadanal and P. Gonçalves, *arXiv Prepr. arXiv1702.03276,* (2017).

[19] A. Mishev, *ISRN High Energy Phys.,* 2012(2012) 1–12.

[20] A. A. Ivanov, S. P. Knurenko, and I. Y. Sleptsov, *New J. Phys.,(*2009) 11.

[21] S. Ostapchenko, *arXiv Prepr. hep-ph/0501093,*(2005).

[22] M. Ohishi et al., *J. Phys. G Nucl. Part. Phys.,* 48 (2021) 75201.